iScience, Volume *23*

Supplemental Information

Anode-Driven Controlled Release of Cathodic Fuel via pH Response for Smart Enzymatic Biofuel Cell

Panpan Gai, Chengcheng Gu, Xinke Kong, and Feng Li

Supporting Information

Transparent Methods

Materials and Reagents. Flavin adenine dinucleotide (FAD)-depended glucose dehydrogenase (GDH) was purchased from Toyobo Co., Ltd. (Japan). 2-Methylimidazole was obtained from Adamas Reagent Co., Ltd. 1-Ethyl-3-(3-dimethyl-aminopropyl) carbodiimide hydrochloride (EDC), *N*-hydroxysuccinimide (NHS), and 3-triethoxysilylpropylamine (APTES) were all purchased from Sigma-Aldrich (St. Louis, MO, U.S.A.). Zinc acetate and chloroauric acid ($HAuCl_4 \cdot 4H_2O$) were commercially available from Shanghai Chemical Reagent Co., Ltd. (Shanghai, China). β-$_D$-Glucose was obtained from Tokyo Chemical Industry Co., Ltd. (Japan). AuNPs were prepared according to the literature by adding a sodium citrate solution to a boiling $HAuCl_4$ solution.(Li et al. 2010) All reagents were of analytical grade and were used as received without further purification. Ultrapure water (resistivity >18.2 MΩ cm at 25°C) obtained from a Milli-Q water purification system (Millipore Corp, Bedford, MA, U.S.A.) was used for all the experiments.

Apparatus. Transmission electron microscopy (TEM) images were recorded on an HT7700 microscope (Hitachi, Japan) operated at 100 kV. Scanning electron microscopy (SEM)-energy dispersive spectroscopy (EDS) was measured on a JEOL 7500F SEM (Hitachi, Japan). X-ray diffraction (XRD) patterns were recorded from a D8 ADVANCE (Bruker, Germany). Electrochemical impedance spectroscopy (EIS) was carried out on an Autolab PGSTAT 302N electrochemical analyzer (Metrohm Autolab, The Netherlands), in which the frequency range was 0.1 Hz-100 kHz, and the electrolyte solution was 2.5 mM of $[Fe(CN)_6]^{3-}$/$[Fe(CN)_6]^{4-}$ probe solution. Cyclic voltammetry (CV), differential pulse voltammetry (DPV), linear sweep voltammetry (LSV), and the open-circuit voltage (E^{OCV}) of EBFC measurements were performed on a CHI 660E

electrochemical workstation (Shanghai CH Instrument Co., China) using a three-electrode system: the prepared anode or cathode a Pt wire and an Ag/AgCl were used as the working electrode, the counter electrode, the reference electrode, respectively. All experiments were carried out at room temperature (25 ± 1°C).

Synthesis of $[Fe(CN)_6]^{3-}$@ZIF-8. Briefly, 1.4 M of 2-methylimidazole and 50 mM of zinc acetate were dissolved in ultrapure water with stirring gently at room temperature. Then, 3 mM of $[Fe(CN)_6]^{3-}$ was added quickly and stirred for 2 h. During this process, $[Fe(CN)_6]^{3-}$ could be encapsulated in the ZIF-8. Afterwards, the mixture was centrifuged (6000 rpm, 5 min) and washed with ultrapure water at least three times to remove the unloaded $[Fe(CN)_6]^{3-}$. Finally, the obtained $[Fe(CN)_6]^{3-}$@ZIF-8 was resuspended into ultrapure water and stored at 4°C for further use.

Preparation of the Positively Charged Cathode and the GDH/AuNPs Anode. The washed indium tin oxide (ITO) was immersed in 1 mM of APTES solution for 5 h at room temperature. Then excess APTES was rinsed with ultrapure water. After these pretreatment procedures, a positively charged cathode was obtained.(Gai et al. 2017) Meanwhile, 30 μL of the prepared AuNPs (50 nM) was coated on the surface of the ITO electrode and dried at 37°C for 2 h. Subsequently, the substrate electrode was immersed in the solution containing 10 mg mL^{-1} of EDC/NHS for 30 min to activate the carboxyl group of AuNPs. After being rinsed with ultrapure water to eliminate excess EDC and NHS, the activated electrode was incubated with 20 μL of GDH solution at 4°C overnight to obtain the GDH/ AuNPs anode.

Fabrication of EBFC. The anode-driven membrane-less EBFC was constructed by using the GDH/AuNPs anode and the positively charged cathode, and operated at room temperature. The supporting electrolyte was 1 mL of 10 mM NaCl solution (pH 7.4) containing 100 μL of $[Fe(CN)_6]^{3-}$

@ZIF-8. The E^{OCV} of EBFC was tested by connecting the anode and cathode placed in the electrolytic cell. Polarization curves of the EBFC were measured by linear sweep voltammetry starting from the open-circuit value at a scan rate of 10 mV s^{-1}. The relationship of power output and the current was calculated based on the polarization curve by the formula of $P=UI$. The as-proposed EBFC was stored at 4℃ when not in use.

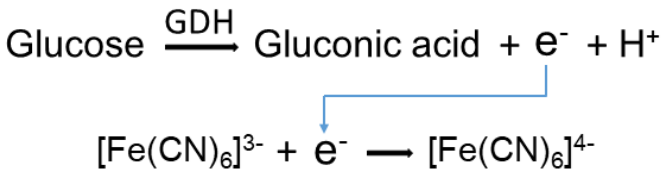

Equation S1. Illustration of the oxidation of glucose and the reduction of $[Fe(CN)_6]^{3-}$, related to Scheme 1.

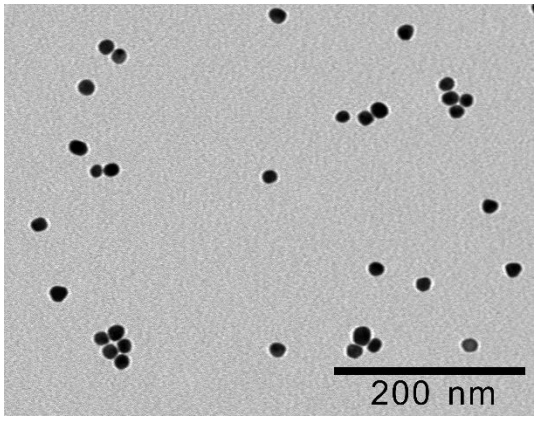

Figure S1. TEM image of AuNPs, related to Figure 1.

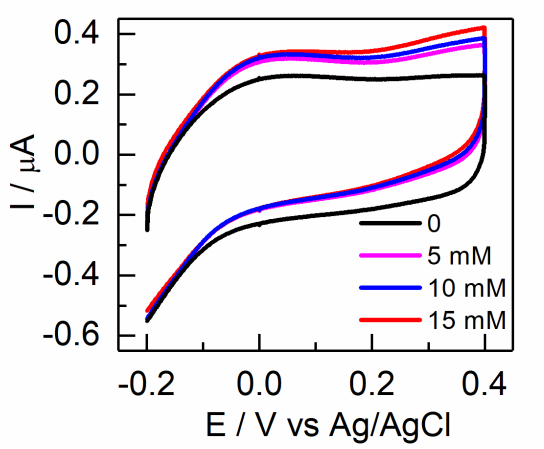

Figure S2. Study of the Anode, related to Figure 1. CVs of the GDH/AuNPs/ITO anode in 10 mM NaCl solution (pH 7.4) with different glucose concentrations.

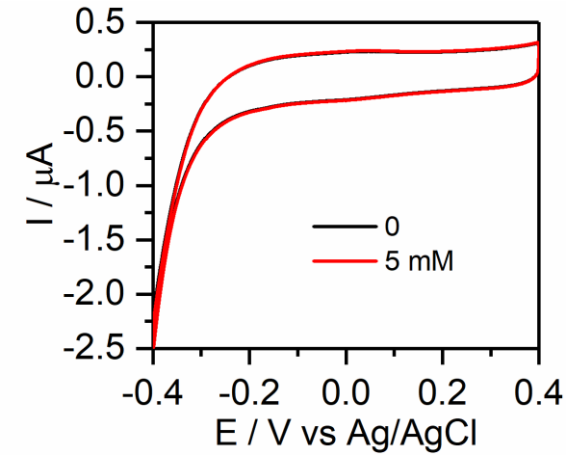

Figure S3. Study of the Anode, related to Figure 1. CVs of the AuNPs/ITO in 10 mM NaCl solution (pH 7.4) with different glucose concentrations.

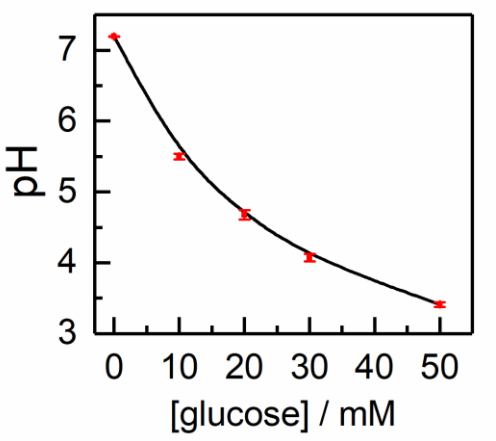

Figure S4. The relationship between pH current values and different glucose concentrations, related to Figure 3. Standard deviation was obtained from three independent measurements.

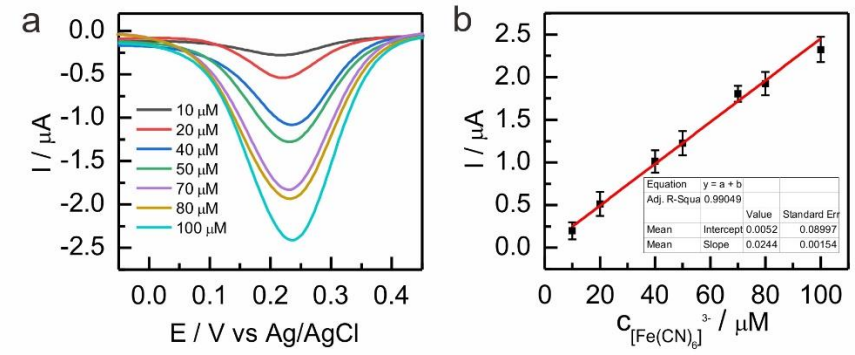

Figure S5. The Relationship Between Current Value and $[Fe(CN)_6]^{3-}$ Concentration, related to Figure 3. (a) DPV curves of the different $[Fe(CN)_6]^{3-}$ concentrations. (b) The linear relationship between current value and $[Fe(CN)_6]^{3-}$ concentration from 10 to 100 μM. Standard deviation was obtained from three independent measurements.

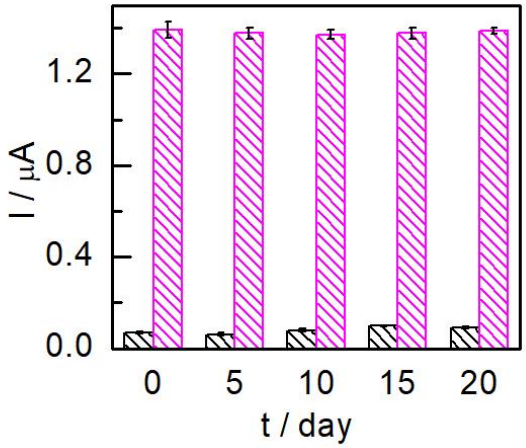

Figure S6. Stability Analysis, related to Figure 3. Stability analysis of the $[Fe(CN)_6]^{3-}$@ZIF-8 nanocarriers in the presence and absence of 50 mM glucose concentration in 20 days. Standard deviation was obtained from three independent measurements.

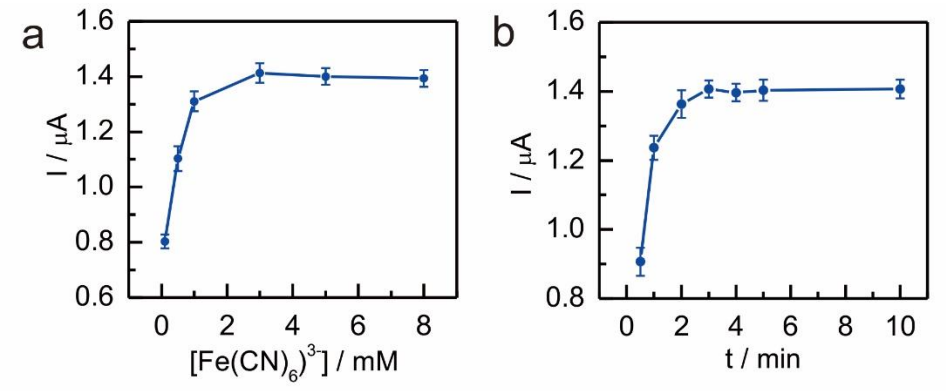

Figure S7. Optimization of $[Fe(CN)_6]^{3-}$ Concentration and the Release Time, related to Figure 3. Effect of (a) $[Fe(CN)_6]^{3-}$ concentration, (b) ZIF-8@$[Fe(CN)_6]^{3-}$ release time. Standard deviation was obtained from three independent measurements.

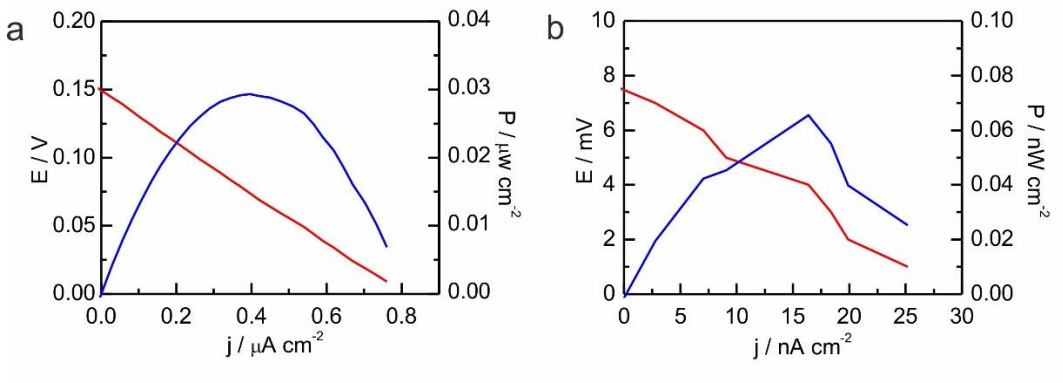

Figure S8. Comparison of Different EBFCs, related to Figure 4. The polarization curves and power output curves of the EBFCs with (a) or without (b) membrane responses with the same concentrations of glucose (50 mM) and $[Fe(CN)_6]^{3-}$ (58.5 μM).

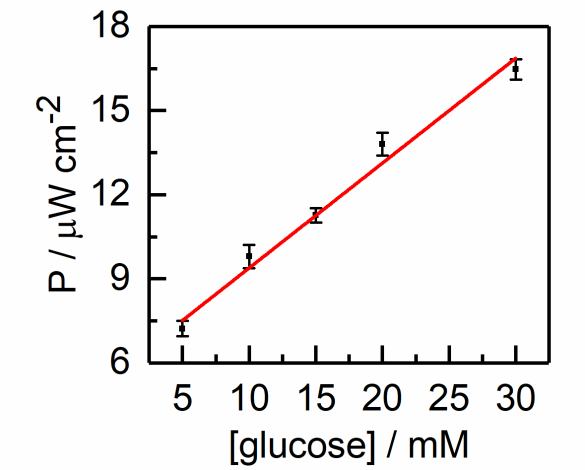

Figure S9. Investigation of the Linear Relationship between Power Output and Glucose Concentration, related to Figure 4. The linear relationship between power output and glucose concentration from 5 to 30 mM. Standard deviation was obtained from three independent measurements.

Gai, P.P., Gu, C.C., Li, H.Y., Sun, X.Z., Li, F. (2017). Ultrasensitive ratiometric homogeneous electrochemical microRNA biosensing via target-triggered Ru(III) release and redox recycling. Anal. Chem. *89*, 12293-12298.

Li, F., Feng, Y., Dong, P., Tang, B. (2010). Gold nanoparticles modified electrode via a mercapto-diazoaminobenzene monolayer and its development in DNA electrochemical biosensor. Biosens. Bioelectron. *25*, 2084-2088.